UC Riverside
UC Riverside Previously Published Works

Title
Targeting Viral Proteostasis Limits Influenza Virus, HIV, and Dengue Virus Infection

Authors
Heaton, Nicholas S
Moshkina, Natasha
Fenouil, Romain
et al.

Immunity

Targeting Viral Proteostasis Limits Influenza Virus, HIV, and Dengue Virus Infection

Graphical Abstract
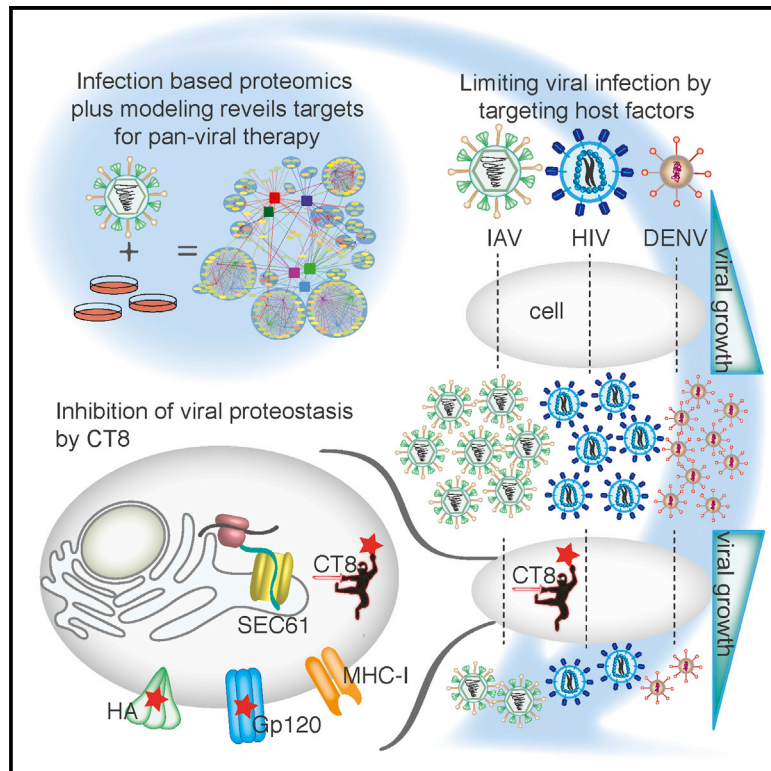
Authors

Nicholas S. Heaton,
Natasha Moshkina, Romain Fenouil, ...,
Jack Taunton, Peter Palese,
Ivan Marazzi

Correspondence

ivan.marazzi@mssm.edu

In Brief

Viruses are obligate parasites dependent on the host cell machinery. Using infection-based proteomics, biochemistry, and mathematical modeling, Marazzi and colleagues reveal that targeting host factors controlling essential cellular functions can provide broad-spectrum antiviral effects. Loss-of-function and chemical inhibition of one such factor, Sec61, inhibited influenza, HIV, and dengue virus replication.

Highlights

- Generated replication-competent, tagged influenza viruses

- Constructed human-influenza interactome network during an infection

- Mathematical modeling revealed host targets for pan-viral inhibition

- Sec61 inhibition alters viral proteostasis and suppresses viral replication

CrossMark

CellPress

Targeting Viral Proteostasis Limits Influenza Virus, HIV, and Dengue Virus Infection

Nicholas S. Heaton,[1,10] Natasha Moshkina,[1,2,10] Romain Fenouil,[3] Thomas J. Gardner,[1] Sebastian Aguirre,[1] Priya S. Shah,[5] Nan Zhao,[1,2] Lara Manganaro,[1] Judd F. Hultquist,[5] Justine Noel,[1,2] David H. Sachs,[3] Jennifer Hamilton,[1] Paul E. Leon,[1] Amit Chawdury,[6,7,8] Shashank Tripathi,[1] Camilla Melegari,[1,2] Laura Campisi,[1,2] Rong Hai,[1] Giorgi Metreveli,[1,2] Andrea V. Gamarnik,[9] Adolfo García-Sastre,[1,2,4] Benjamin Greenbaum,[6,7,8] Viviana Simon,[1,2] Ana Fernandez-Sesma,[1,2] Nevan J. Krogan,[5] Lubbertus C.F. Mulder,[1,2] Harm van Bakel,[3] Domenico Tortorella,[1] Jack Taunton,[5] Peter Palese,[1] and Ivan Marazzi[1,2,*]

[1]Department of Microbiology, Icahn School of Medicine at Mount Sinai, New York, NY 10029-6574, USA
[2]Global Health and Emerging Pathogens Institute, Icahn School of Medicine at Mount Sinai, New York, NY 10029-6574, USA
[3]Department of Genetics and Genomic Sciences, Icahn School of Medicine at Mount Sinai, New York, NY 10029-6574, USA
[4]Division of Infectious Diseases, Department of Medicine, Icahn School of Medicine at Mount Sinai, New York, NY 10029-6574, USA
[5]Department of Cellular and Molecular Pharmacology, University of California, San Francisco, San Francisco, CA 94158-2140, USA
[6]Tisch Cancer Institute, Icahn School of Medicine at Mount Sinai, New York, NY 10029-6574, USA
[7]Division of Hematology and Oncology, Department of Medicine, Icahn School of Medicine at Mount Sinai, New York, NY 10029-6574, USA
[8]Department of Pathology, Icahn School of Medicine at Mount Sinai, New York, NY 10029-6574, USA
[9]Fundación Instituto Leloir-CONICET, Avenida Patricias Argentinas 435, Buenos Aires 1405, Argentina
[10]These authors contributed equally to this work
*Correspondence: ivan.marazzi@mssm.edu
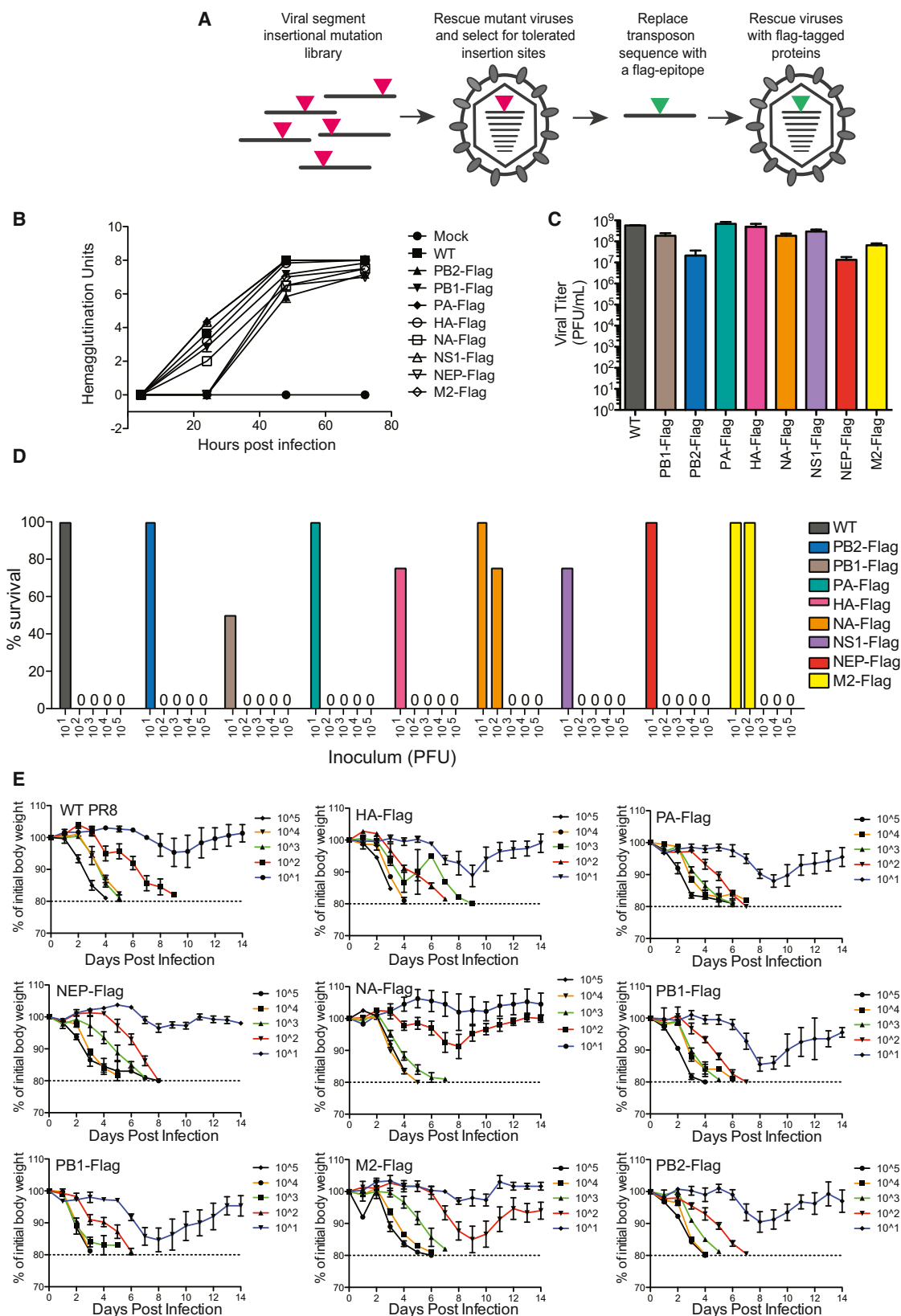http://dx.doi.org/10.1016/j.immuni.2015.12.017

SUMMARY

Viruses are obligate parasites and thus require the machinery of the host cell to replicate. Inhibition of host factors co-opted during active infection is a strategy hosts use to suppress viral replication and a potential pan-antiviral therapy. To define the cellular proteins and processes required for a virus during infection is thus crucial to understanding the mechanisms of virally induced disease. In this report, we generated fully infectious tagged influenza viruses and used infection-based proteomics to identify pivotal arms of cellular signaling required for influenza virus growth and infectivity. Using mathematical modeling and genetic and pharmacologic approaches, we revealed that modulation of Sec61-mediated cotranslational translocation selectively impaired glycoprotein proteostasis of influenza as well as HIV and dengue viruses and led to inhibition of viral growth and infectivity. Thus, by studying virus-human protein-protein interactions in the context of active replication, we have identified targetable host factors for broad-spectrum antiviral therapies.

INTRODUCTION

Influenza A virus (IAV) is a major human pathogen and a global health threat (Shaw and Palese, 2013). Due to limited genomic space, IAV proteins have been shown to perform a multitude of functions in the host cell (Hale et al., 2008; Paterson and Fodor, 2012; Portela and Digard, 2002). As such, a molecular understanding of how each viral protein co-opts and interferes with

cellular processes during infection is critical for the elucidation of mechanisms of pathogenesis and for the development of novel therapeutic strategies. To gain insight into virus-host protein interactions, studies have been performed with yeast 2-hybrid systems, complementation assays, or affinity purification of epitope-tagged viral proteins transfected into cells (Bradel-Tretheway et al., 2011; de Chassey et al., 2013; Gorai et al., 2012; Guan et al., 2012; Jorba et al., 2008; Lin et al., 2012; Mayer et al., 2007; Munier et al., 2013; Ngamurulert et al., 2009; Shapira et al., 2009; Tafforeau et al., 2011). Although these approaches have indicated potential cellular factors targeted by viral proteins, they are limited by the fact that the mere expression of influenza proteins does not recapitulate key physiological aspects of the host-virus battleground. Essentially, these studies do not take into account the context of an infectious event, during which the dynamics between host and virus are co-regulated by the viral life cycle and the antiviral state that is established in the infected cell. As a result, these studies fail to capture (1) activation of signaling networks and expression of cellular proteins in response to viral infection, (2) large-scale modification of cellular structures and organelles (promyelocytic leukemia [PML] bodies, mitochondria, replication factories) induced by the infection, (3) cooperation between viral proteins in performing pivotal functions of the viral life cycle (transcription and replication). In this report, we have described an approach for generating fully infectious viruses that harbor affinity-purification tags and allow the study of virus-host protein interactions during active viral replication. We used this system to generate an interactome map of host and influenza virus proteins (and protein complexes) during an active infection. We identified, and validated experimentally, pivotal arms of host signaling utilized by the influenza virus to sustain its life cycle.

Guided by the infection proteomic-network analysis, we focused on ER-mediated processes, and specifically on Sec61-mediated regulation of cotranslational translocation and protein

A

Viral segment insertional mutation library → Rescue mutant viruses and select for tolerated insertion sites → Replace transposon sequence with a flag-epitope → Rescue viruses with flag-tagged proteins

B

Legend:
- Mock
- WT
- PB2-Flag
- PB1-Flag
- PA-Flag
- HA-Flag
- NA-Flag
- NS1-Flag
- NEP-Flag
- M2-Flag

Y-axis: Hemagglutination Units
X-axis: Hours post infection

C

Y-axis: Viral Titer (PFU/mL)
X-axis categories: WT, PB1-Flag, PB2-Flag, PA-Flag, HA-Flag, NA-Flag, NS1-Flag, NEP-Flag, M2-Flag

D

Y-axis: % survival
X-axis: Inoculum (PFU)

Legend:
- WT
- PB2-Flag
- PB1-Flag
- PA-Flag
- HA-Flag
- NA-Flag
- NS1-Flag
- NEP-Flag
- M2-Flag

E

Panels: WT PR8, HA-Flag, PA-Flag, NEP-Flag, NA-Flag, PB1-Flag, PB1-Flag, M2-Flag, PB2-Flag

Each with legend: 10^5, 10^4, 10^3, 10^2, 10^1

Y-axis: % of initial body weight
X-axis: Days Post Infection

(legend on next page)

folding. We show that partial depletion and chemical inhibition of Sec61 specifically affect biosynthesis of influenza virus proteins HA (and NA) and, in turn, viral biogenesis. Using loss-of-function screening (dengue virus [DENV]) and mathematical modeling of how proteins segregate in interaction networks during infection with different pathogens (HIV and influenza virus), we show that Sec61 partial depletion and chemical inhibition suppresses HIV and DENV replication with little to no effect on cellular proteostasis. We discuss the rationale of targeting essential cellular function as a strategy for developing pan-antiviral therapies.

RESULTS

Fully Infectious, Flag-Tagged Influenza Viruses Generated by Mutagenesis

In order to produce a global model of the virus-host relationship in the context of an active viral infection, we developed a system of generating fully infectious reporter viruses. In brief, we mutagenized IAV segments (PB1, PB2, PA, HA, NA, NS1, NEP, M2, M1, NP) to encode a Flag epitope in transposition-prone regions of the viral segments (Figure 1A) (Heaton et al., 2013b). The IAV reverse-genetics system (García-Sastre and Palese, 1993) utilized for rescuing mutant viruses led to successful recovery of tagged and replicating virus for eight of the ten major viral proteins of the H1N1 PR8 influenza strain, A/Puerto Rico/8/1934 (Figure S1A). Viruses harboring tagged versions of the highly conserved matrix protein M1 or the nucleoprotein NP were not recovered, probably due to the high number of constraints on the structures of these proteins (Heiny et al., 2007; Noton et al., 2007; Portela and Digard, 2002). We tested the replication of the tagged viruses by performing multi-cycle growth curves on Madin-Darby Canine Kidney Epithelial Cells (MDCK) cells (Figure 1B). Although we observed a slight delay in the kinetics of growth with the PB2-Flag, M2-Flag, and NEP-Flag viruses relative to wild-type (WT) and the other tagged viruses, the plaque-forming units at 48 hr post-infection indicated that the tagged viruses displayed wild-type (PB1-Flag, PA-Flag, NS1-Flag, HA-Flag, NA-Flag) or near wild-type (PB2-Flag, M2-Flag, and NEP-Flag) titers (Figure 1C). To test whether our compendium of Flag viruses retained the tagged segments, we sequenced viruses after several (2–4) rounds of viral-stock amplification and found that the tags were retained, indicating that the insertion sites were stable (Figure S1B). To assess whether the tagged segments were expressed and if viral protein complexes were formed during Flag-tagged viral infection, we set up an affinity purification of Flag-PB2 after infecting A549 human lung epithelial cells. This led to the recovery of PB2, PA, PB1, and NP (Figure S1C), indicative of the isolation of biologically relevant viral ribonucleoprotein complexes (vRNPs). Finally, we tested viral fitness in an animal model of infection. BALB/c mice were infected with doses ranging from 10–10^5 PFUs, and analysis of morbidity and mortality indicated that all the viruses had comparable median lethal doses (Figure 1D), even in cases where the kinetics of weight loss were slightly reduced (Figure 1E). Taken together, the stability and replication properties of the Flag-tagged viruses provided us with useful tools for characterizing the molecular mechanisms of viral infection.

Interactions between Influenza Virus and Host Proteins during Infection

We then aimed to generate a map of host-influenza protein interactions during an active infection. We infected the human lung epithelial cell line A549 with each of the eight Flag-tagged viruses (Figure S2A, schematic of the experimental strategy) and used both untagged WT virus as well as Flag-tagged green fluorescent protein (GFP) as controls. Flag-affinity-purified preparations of each viral bait, along with the co-immunoprecipitated host and viral factors, were then submitted for protein identification via mass spectrometry with previously published protocols optimized for the identification of viral-host interactions (Jäger et al., 2011). Key to such analysis was the use of (1) biologically replicated datasets to control for reproducibility and specificity, (2) interaction datasets originating from wild-type (non-tagged) virus and Flag-GFP expression, which both removed all the resident and infection-induced proteins that bound non-specifically to the Flag antibody or resin, (3) stringent statistical criteria for data analysis (Mist score $\geq$ 0.9; see Tables S1–S4 for raw data and processed data, Supplemental Experimental Procedures for statistical analysis, and Figures S2B–S2D for visual representation of the stringency of the cutoff with regard to known false-positive-abundant contaminants and published datasets (Watanabe et al., 2014)]. We thus identified a set of high-confidence interactors and generated an influenza-host interactome during active infection (Figure 2A; Figures S2E and S3; Tables S1–S3; and Table S4 for additional biased filtering based on biological rationales).
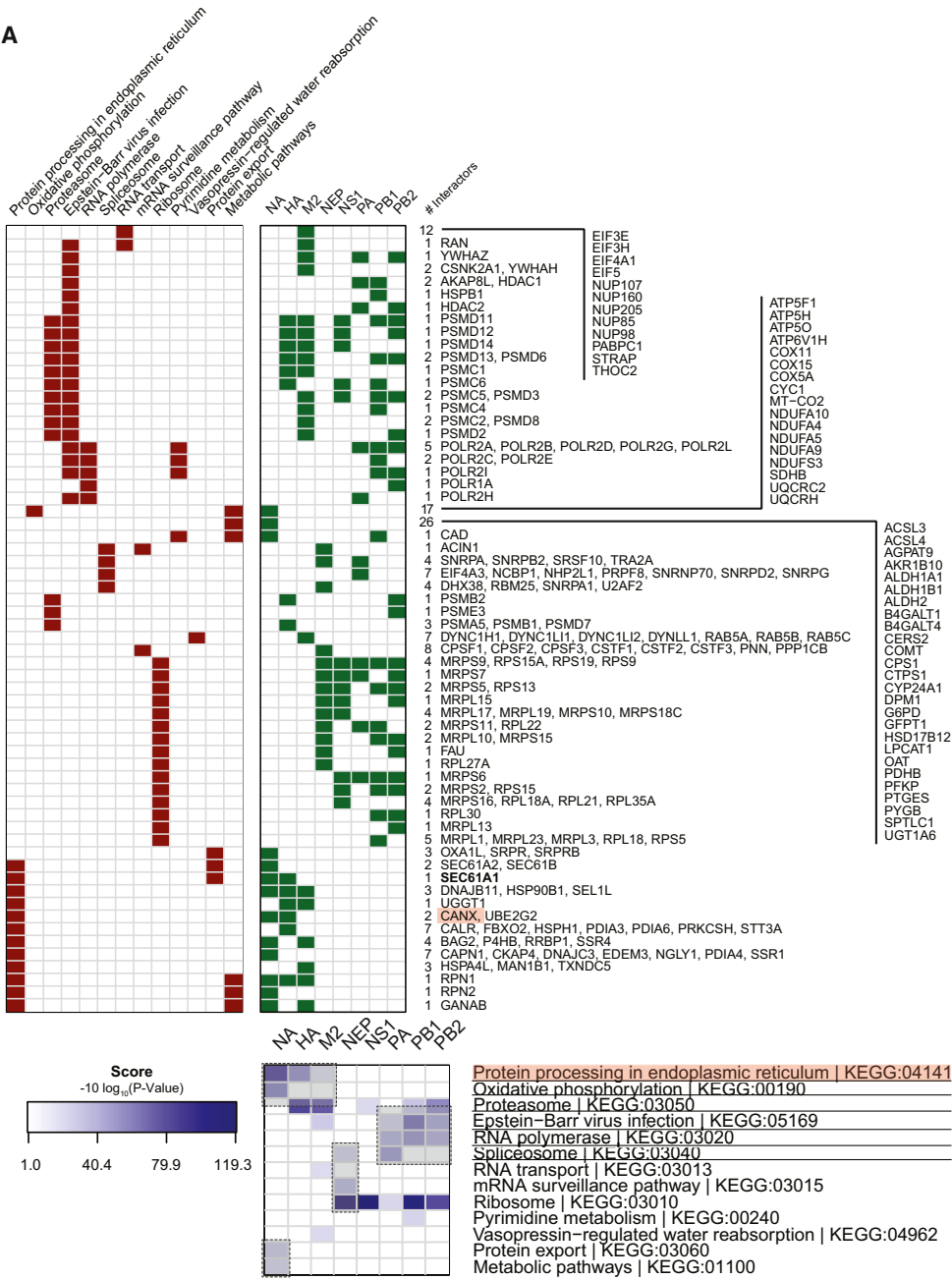
The proteome interaction network revealed several findings. First, we detected common sets of host proteins that were immunoprecipitated by distinct viral proteins (Figure 2A and Figure S2E). This reflected the physiological formation of vRNPs during infection, as suggested by the relationship between viral proteins and known cellular functions (Figure 2A GO category, blue boxes) and complexes (Figure S2E). This indicated the main "nodes" of interaction of influenza with the cellular proteome.

Second, we detected potentially novel interactions, such as those between viral Polymerase complex (vPol) and the CTCF complex, which controls the 3D structure of the genome. This interaction suggests that chromatin insulators could play a role in controlling viral replication and/or antiviral gene expression. We also detected the targeting of important cellular complexes such as the SPT complex, which regulates the synthesis of
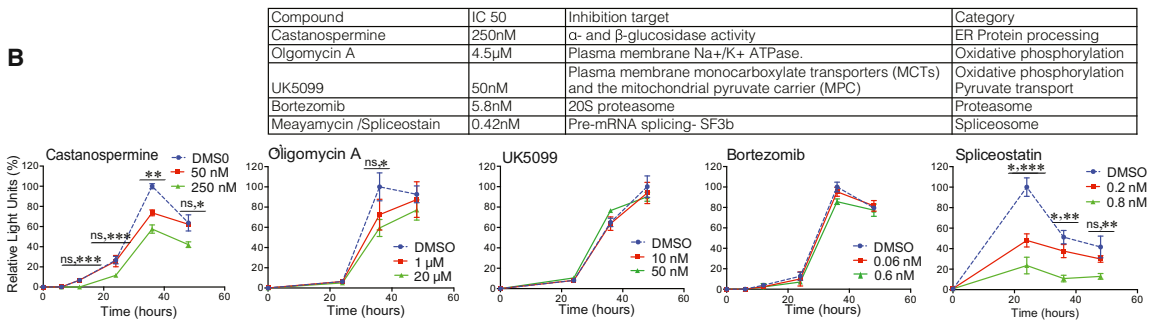
Figure 1. Development of Fully Infectious Flag-Tagged Influenza Viruses
(A) Schematic representation of the strategy used for generating the compendium of the Flag-tagged influenza viruses.
(B) MDCK cells were infected at an MOI of 0.001. Multi-cycle viral growth was quantified by a hemagglutination assay at the indicated time points.
(C) Viral titer (PFU) of Flagg-tagged viruses and control at 48 hr after infection. Means and SD are shown.
(D) Percentage survival in BALB/c mice (n = 5) after infection with Flag-tagged viruses.
(E) Morbidity in BALB/c mice (n = 5) after infection with Flag-tagged viruses. 6- to 8-week-old female BALB/c mice were challenged with the indicated doses of virus, and body weight was monitored over a 14 day time course. Means and SD are shown. See also Figure S1.

A

B

Compound	IC 50	Inhibition target	Category
Castanospermine	250nM	α- and β-glucosidase activity	ER Protein processing
Olgomycin A	4.5µM	Plasma membrane Na+/K+ ATPase.	Oxidative phosphorylation
UK5099	50nM	Plasma membrane monocarboxylate transporters (MCTs) and the mitochondrial pyruvate carrier (MPC)	Oxidative phosphorylation Pyruvate transport
Bortezomib	5.8nM	20S proteasome	Proteasome
Meayamycin /Spliceostain	0.42nM	Pre-mRNA splicing- SF3b	Spliceosome

(legend on next page)

sphingolipids and it is co-opted by other viruses (Schneider-Schaulies and Schneider-Schaulies, 2015), and the CCT complex, which regulates protein folding and is targeted by a different influenza strain (Fislová et al., 2010)] (Figure S2E). These results suggest that inhibition of these cellular complexes might represent strategies for interspecies and pan-viral inhibition. Third, our analysis confirmed previous findings, including the targeting of RNAPII transcriptional complexes by the influenza replicative machinery (PA, PB1, and PB2), that underscored the importance of cellular transcription for viral ribogenesis (Amorim et al., 2007; Engelhardt et al., 2005) as well as the interaction of M2 and NA viral proteins with components of the cellular respiration complex (Alsuwaidi et al., 2013; Ritter et al., 2010) (Figure S3). Fourth, our data allowed for a comparison between previously generated global proteomic-interaction datasets in the absence of infection (Watanabe et al., 2014) (Figures S2B and S2D). To validate the role of host pathways during infection, we pharmacologically inhibited proteins controlling specific targeted complexes identified by hierarchical functional clustering of host pathways co-opted by viral proteins (blue boxes in Figure 2A GO category; also Table S2). We measured viral replication of IAV in A549 cells upon treatment with inhibitors controlling the most statistically significant host pathways identified in Figure 2A (underlined GO category). We used Castanospermine (alpha-glucosidase inhibitor) for endoplasmic reticulum (ER)-processes, UK5099 (MCP pyruvate carrier inhibitor) and Olygomycin A (inhibitor of the Fo subunit of the ATP synthase) for events linked to oxidative phosphorylation; Bortezomil (inhibitor of the 26S proteasome); and Spliceostatin A (SF3B-inhibitor) for spliceosome inhibition. Our results evidenced that targeting of nuclear (SF3B) and cytosolic (alpha-glucosidases) factors can suppress viral replication (Figure 2B) and indicated that cotranscriptional events and host factors controlling protein glycosylation and apical trafficking could be targetable interfaces for antiviral activity (see below).

Sec61A1 Is a Required Host Factor for Influenza Virus Replication

We then decided to characterize in detail the most highly enriched biological pathway of protein processing in the ER (Figure 2A, KEGG pathway analysis; $p = 10^{-9}$) and specifically the heterotrimeric Sec61 complex, which is essential for the biogenesis of most secretory and membrane proteins (Gogala et al., 2014).

Although Sec61 had not been previously studied in the context of influenza-virus infection, it scored in our proteomic analysis as a high-confidence interactor with the viral proteins HA and NA, but not M2 (Figure 3A, Table S3). All three viral membrane proteins most likely require transient association with Sec61

for cotranslational insertion into the ER, but only HA and NA have large glycosylated extracellular domains with complex folding requirements (Braakman et al., 1991; Copeland et al., 1986; Copeland et al., 1988; Daniels et al., 2003; Hebert et al., 2014; Hebert et al., 1997; Saito et al., 1995; Wang et al., 2008). In agreement with this, we also noted that HA and NA, but not M2, bound Calnexin (CANX), a molecular chaperone that physically associates with the Sec61 translocon and assists glycoproteins folding and maturation (Figure 3A) (Caramelo and Parodi, 2008; Lakkaraju et al., 2012; Lynes et al., 2013). These shared attributes, along with (1) unique regulatory mechanisms of protein maturation occurring during infection (Molinari et al., 2004; Pieren et al., 2005), (2) the possibility of prolonged substrate-specific interaction with the translocon required for protein folding and oligomeric assembly (Conti et al., 2015; Fayadat and Kopito, 2003), and (3) the fact that viruses must biosynthesize large amounts of proteins in a short time frame of infection led us to hypothesize, first, that Sec61A1 might be an important host factor controlling influenza biogenesis and, second, that Sec61 transient inhibition could be well tolerated by the cell but not by the virus.

We first validated the IAV and HA-Sec61 translocon interaction by density-gradient fractionation of post-nuclear lysates derived from IAV-infected A549 cells (Figure 3B) and by co-immunoprecipitation (Figure 3C). These results indicated that the interaction of HA with the Sec61 translocon was occurring during, and possibly after, the obligate step of co-translational translocation into the ER.

We then assessed the effect of Sec61 perturbation on viral replication by transient and partial depletion of Sec61 via small interfering RNA (siRNA) or by chemical inhibition. We achieved the latter by using a small-molecule inhibitor (CT8) that can specifically affect Sec61-dependent cotranslational translocation depending on the physicochemical properties of a given substrate (Besemer et al., 2005; Garrison et al., 2005; Kalies and Römisch, 2015; Mackinnon et al., 2014).

As shown in Figure 3D (left panel), increasing concentrations of the inhibitor CT8 led to a dose-dependent decrease in the release of IAV infectious viral particles with minimal effects on cellular viability (Figure 3D, right panel). Similarly, siRNA knockdown of Sec61A1 led to a reduction in the levels of Sec61 (Figures S4A and S4B) and a concomitant reduction in the release of infectious IAV particles (Figure S4C) with no major effects on cellular viability (Figure S4D) or viral entry (Figure S4E).

To determine whether the reduced infectivity in the presence of CT8 was caused by reduced HA expression, we performed orthogonal biotinylation and subsequent purification of cell-surface HA (Figure 3E, upper panel). We performed this experiment in both WT and Sec61A1 mutant cells that lacked CT8 sensitivity

---

Figure 2. Proteomics of Infectious Influenza Virus Proteins and Validation of Targeted Pathways

(A) The interacting virus proteins (green) and KEGG pathway membership (red) are indicated for each host protein. KEGG pathway enrichment scores ($-10 \log_{10}$ p value) for interactors with each viral protein are indicated in blue (see color scale). Boxes highlight clusters of interactions.

(B) A549 cells were treated with the inhibitors Castanospermine, Oligomycin A, UK5099, Bortezomib, and Spliceostatin in a range of concentrations where no cytotoxicity was detected, and viral growth was estimated by Renilla luciferase assay at 12, 24, 36, and 48 hr after infection. Data represent means and SD of three biological replicates. Note that it has also been suggested that a high concentration of UK5099 inhibits mitochondrial respiration (Divakaruni and Murphy, 2012; Halestrap, 2012). Luciferase read outs are normalized to DMSO. Statistical analysis between datasets was performed with a two-tailed Student's t test. For all panels, $*p \leq 0.05$, $**p \leq 0.005$, $***p \leq 0.0005$, and ns = not significant (indicated in the order: lower concentration first, followed by higher concentration of inhibitors). See also Figures S2 and S3.
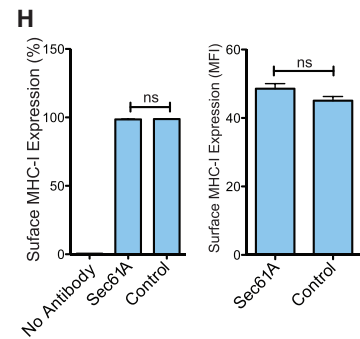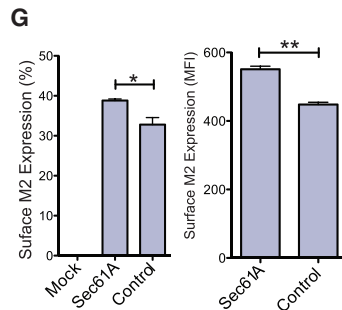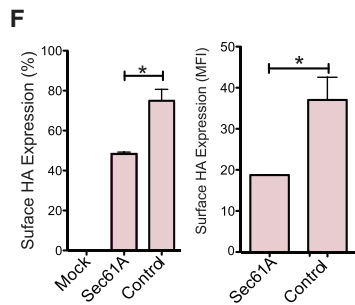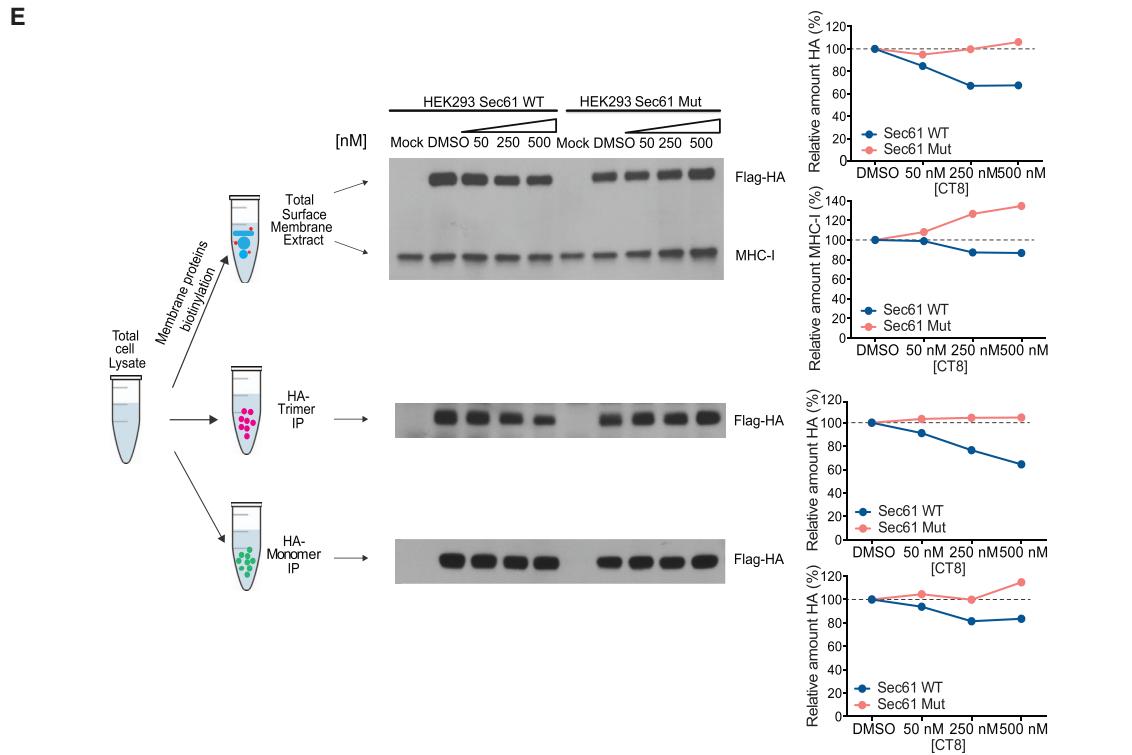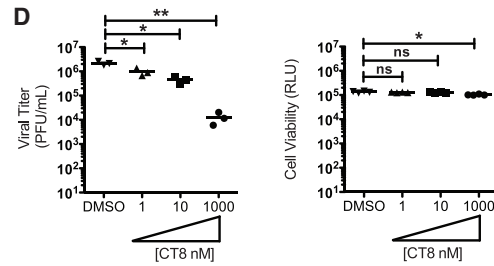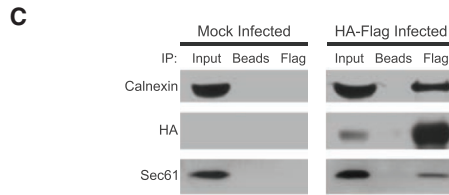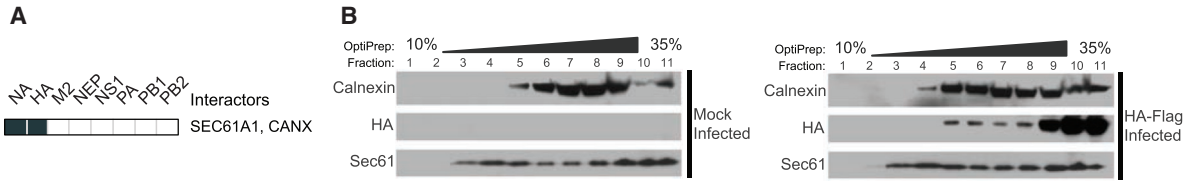
(legend on next page)

(Mackinnon et al., 2014). Our results showed that, upon infection, CT8 treatment decreased HA membrane protein in WT cells but not in mutant cells (Figure 3E, upper panel). These data genetically linked Sec61A1 with the specificity of HA inhibition by CT8.

Similarly, flow-cytometry analysis revealed that transport of HA to the plasma membrane was significantly reduced after treatment with siRNAs targeting Sec61A1 (Figure 3F). For controls, we looked at surface levels of M2, another virally encoded transmembrane protein that is transported from the ER to the plasma membrane and the host MHC-I protein, a type I membrane protein that utilizes the Sec61 translocon for membrane insertion (Schnell and Hebert, 2003). Strikingly, M2 and MHC-I displayed no reduction in surface expression under Sec61A1 depletion (Figures 3G and 3H). These results suggest that some viral glycoproteins, possibly those, such as HA and NA, that have prolonged interaction with Sec61 (Figure 3A), are more sensitive to translocon inhibition than other membrane proteins. These results were further supported by metabolic chase analysis monitoring the initial step of HA synthesis and folding (Braakman et al., 1991). This analysis revealed a delay in glycan maturation in CT8-treated cells (Figures S4F and S4G) and in Sec61A1-depleted cells compared to controls (Figure S4H).

Finally, because the physiologically active form of HA is trimeric, we assessed HA oligomerization with respect to Sec61 protein levels. Control and CT8-treated WT and Sec61A1 mutant cells were infected with IAV HA-Flag viruses, and immunoprecipitation of monomeric and homo-trimeric HA followed (Figure 3E, middle and lower panels). The results revealed that the diminished amount of surface HA caused by CT8 is primarily the result of reduced trimer formation (Figure 3E, middle panel), which occurs to a greater extent than reduced monomer formation (Figure 3E, lower panel). Overall, these data indicate that diminished cellular amounts or chemical perturbation of Sec61 results in the temporal delay of the physiological processing and maturation of HA and results in diminished functional HA surface expression and viral infectivity. This interpretation is supported by the fact that the rate of folding of HA is dependent on cellular factors (Braakman et al., 1991). Delayed folding will then result in a decrease of HA, which is more evident at the trimeric level because oligomerization assembly approximates second-order reactions (Grasberger et al., 1986).

Mathematical Modeling of Influenza and HIV Interactions

Because different viruses often target common host proteins, we compared our proteomic datasets for influenza to those previously published for HIV (Jäger et al., 2012). We mathematically inferred (Menche et al., 2015) the distance relatedness of host interaction partners targeted by the two viruses (Figure 4A). Enrichment analysis of the most closely related partners indicated that "protein localization to ER" (Figure 4A, red dots indicating paired interactions) is the most significant process both viruses utilize during infection. Analysis of influenza HA-HIV protein pairwise interactions (see Supplemental Experimental Procedures) prompted the investigation of the HIV glycoprotein (gp)120 as a potential target of Sec61 inhibition.

Sec61 Controls HIV Biogenesis and Can Be Targeted to Suppress HIV Infectivity

We first analyzed gp120 trafficking in the context of Sec61A1 knockdown. siRNA-treated cells were transfected with plasmids encoding full-length HIV-1 clone R7.3 33A expressing GFP in the Nef position (Chakrabarti et al., 2002; Lue et al., 2002), and gp120 surface expression was assessed by flow cytometry with conformation-specific antibodies that recognize gp120 in monomeric (2G12) and trimeric (PG9) forms (Figures S5A and S5B). Our data indicated that, at similar transfection efficiency (Figure S5A), a reduced amount of Sec61 affected the surface detection of gp120 (Figure 4B). The effect was more prominent when cells were probed with the PG9 antibody, consistent with gp120 trimer formation's being particularly sensitive to low Sec61 protein levels in the cell (Figure 4B). Accordingly, impaired surface expression of gp120 also leads to a reduction in HIV-1 infectivity (Figure 4C). These data show that physiological amounts of Sec61A1 protein are important for HIV-1 biogenesis.

We then used chemical inhibition of Sec61 to validate the specific requirement for the Sec61 complex in HIV-1 replication. We performed multi-cycle viral growth experiments by infecting the A3R5.7 T cell line with three different HIV strains in the presence of increasing concentrations of CT8. Growth of all three HIV-1 strains was significantly inhibited (Figure 4D), and there was no major reduction in cellular viability by 7 days after treatment

Figure 3. Sec61A1 Controls HA Surface Expression and Influenza Viral Replication
(A) Schematic depiction of the interaction of influenza proteins with Sec61 and CANX on the basis of KEGG enrichment overrepresented in the ER pathway.
(B) Post-nuclear lysate of A549 cells infected with HA-Flag virus was fractionated over an OptiPrep gradient. Fractions were analyzed via immunoblot for the indicated proteins.
(C) A549 cells were treated with mock virus or infected with HA-Flag-tagged influenza virus. The HA protein was immunoprecipitated with anti-Flag or control beads. Co-immunoprecipitated proteins were detected by immunoblot. A representative of two experiments is shown.
(D) A549 cells were treated with the Sec61 inhibitor CT8 at the indicated concentrations for 2 hr. Effects on viral titer (left) and cellular viability (right) are shown at time point 18 hr.
(E) HEK293 cells that were Ct8 sensitive (WT) or insensitive (Mut) were infected with Flag-HA at an MOI of 3 and treated with indicated concentrations of CT8. Total cell lysates were split in three parts; one was used for isolating total surface membrane proteins and detecting the levels HA and MHC-I by immunoblotting. The other two-thirds were subjected to immunoprecipitation with the HA-specific antibodies that recognize monomers (PY102) or trimers (6F12). Total and trimeric HA were detected by Western blot (WB), and their amounts were analyzed by densitometry quantification done by single-area measurements of the bands. HA and MHC-I amounts at different CT8 concentrations are quantified as percent of samples treated with DMSO. The same film was used for HA detection and quantification. A representative of two experiments is shown.
(F–H) A549 cells were treated with control or Sec61A1 targeting siRNAs. 48 hr after knockdown, cells were infected with wild-type PR8 for 8 hr. Cells were fixed and stained so that surface expression of HA (F), M2 (G), or MHC-I (H) could be detected. The percent of cells positive for expression and the mean fluorescent intensity of positive cells are shown.
For all panels, *p ≤ 0.05, **p ≤ 0.001, and ns = not significant. See also Figure S4.
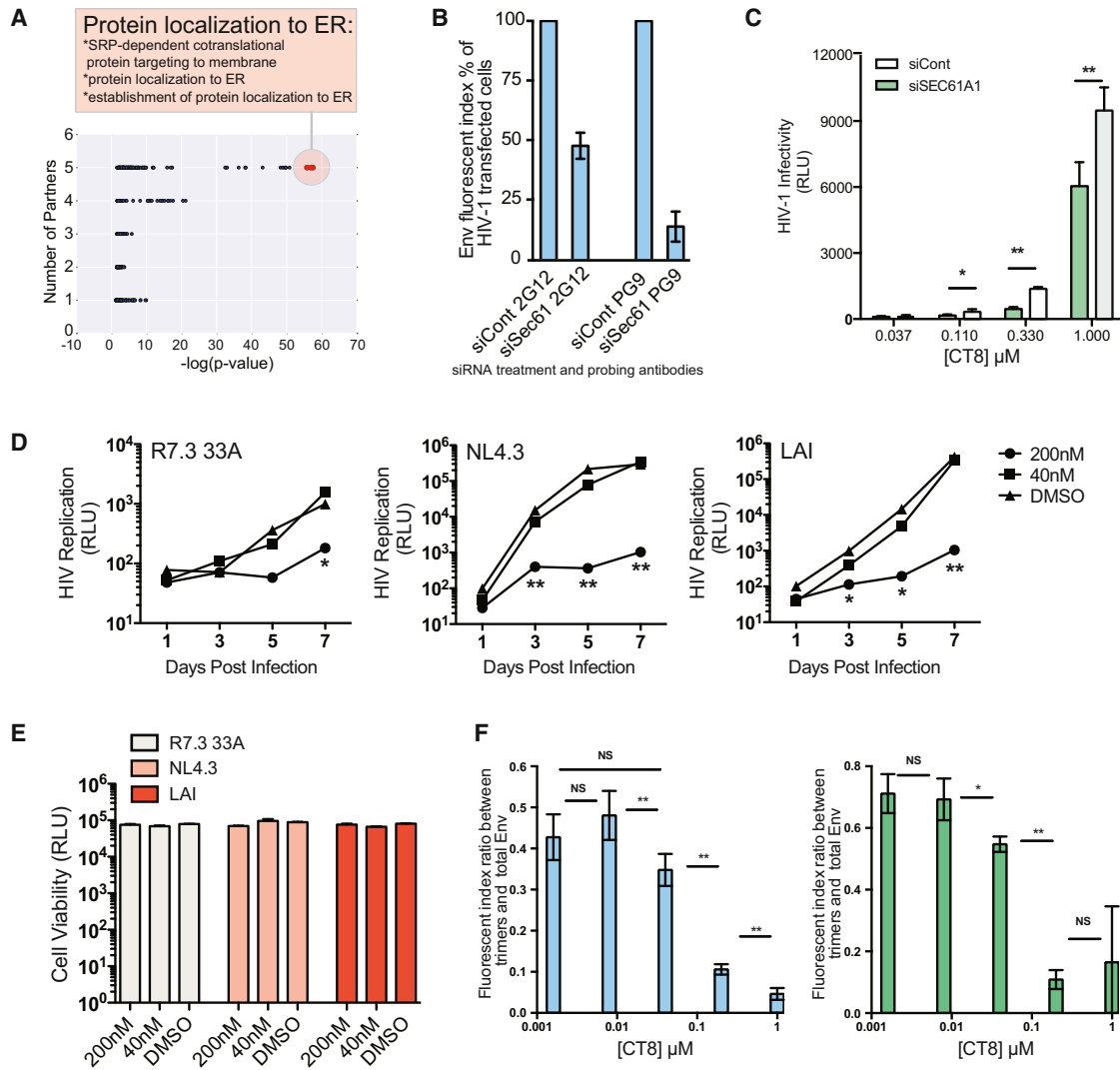
Figure 4. Sec61A1 Controls HIV-1 Env Surface Expression and Viral Replication

(A) Scatterplot containing the gene-ontology categories that applied to the top five most closely related interaction partners. The y axis is the number of paired interaction partners that generated the category ($S_{AB} < 0$), and the x axis is the negative log of the category's average p value across all its generating partners. Red highlights the ontology category related to ER-mediated events.

(B) Full-length HIV-1 genomic constructs expressing GFP were transfected into 293T cells treated with control or Sec61A1 siRNAs. Surface gp120 data are indicated as the fluorescent index of transfected cells (GFP) expressing HIV-1 Env (see Experimental Procedures). Expression in cells treated with control siRNA (SiCont) was set to 100%. HIV-1 Env was probed with the monoclonal antibodies 2G12 (monomeric form) and PG9 (trimeric form). The experiment was performed three times in triplicates.

(C) The infectivity of viruses was determined with 3× serial dilutions of viral supernatants of control and Sec61A1 siRNA-treated cells transfected with full-length HIV-1 and measured with the TZM-bl luciferase reporter cell line (one representative silencing experiment out of three is shown).

(D) Three HIV-1 strains were used for infecting 3×10^5 A3R5 T cells (per well) in the presence of different concentrations the inhibitor CT8. A viral replication growth curve, measured by the infectivity of a fixed volume of viral supernatant harvested at the indicated days, is shown. The experiment was performed in triplicate for each viral strain.

(E) Cellular viability from (C) measured the end point of the experiment (day 7).

(F) HEK293T cells transfected with full-length HIV-1 genomic constructs (R7/3-33A GFP and LAI GFP) were treated with increasing amounts of CT8. Monomeric and trimeric gp120 expression was determined by staining with 2G12 and PG9 antibodies, respectively, followed by flow-cytometry analysis. Results are expressed as the ratio between the fluorescent index of cells expressing trimeric gp120 (probed with PG9) and the fluorescent index of cells expressing momomeric gp120 (probed with 2G12). Three independent experiments were performed for each CT8 concentration and for each viral strain. All error bars represent SD and *p < 0.05, **<0.01. See also Figure S5.

(Figure 4E). Finally, we quantified trimeric versus monomeric gp120 surface expression in the presence of increasing concentrations of CT8. The results of this analysis performed on two viral strains show that the detection of gp120 trimer was inhibited in a dose-dependent manner by CT8 (Figure 4F), and CT8 did not have an impact on cell viability (Figure S5C).
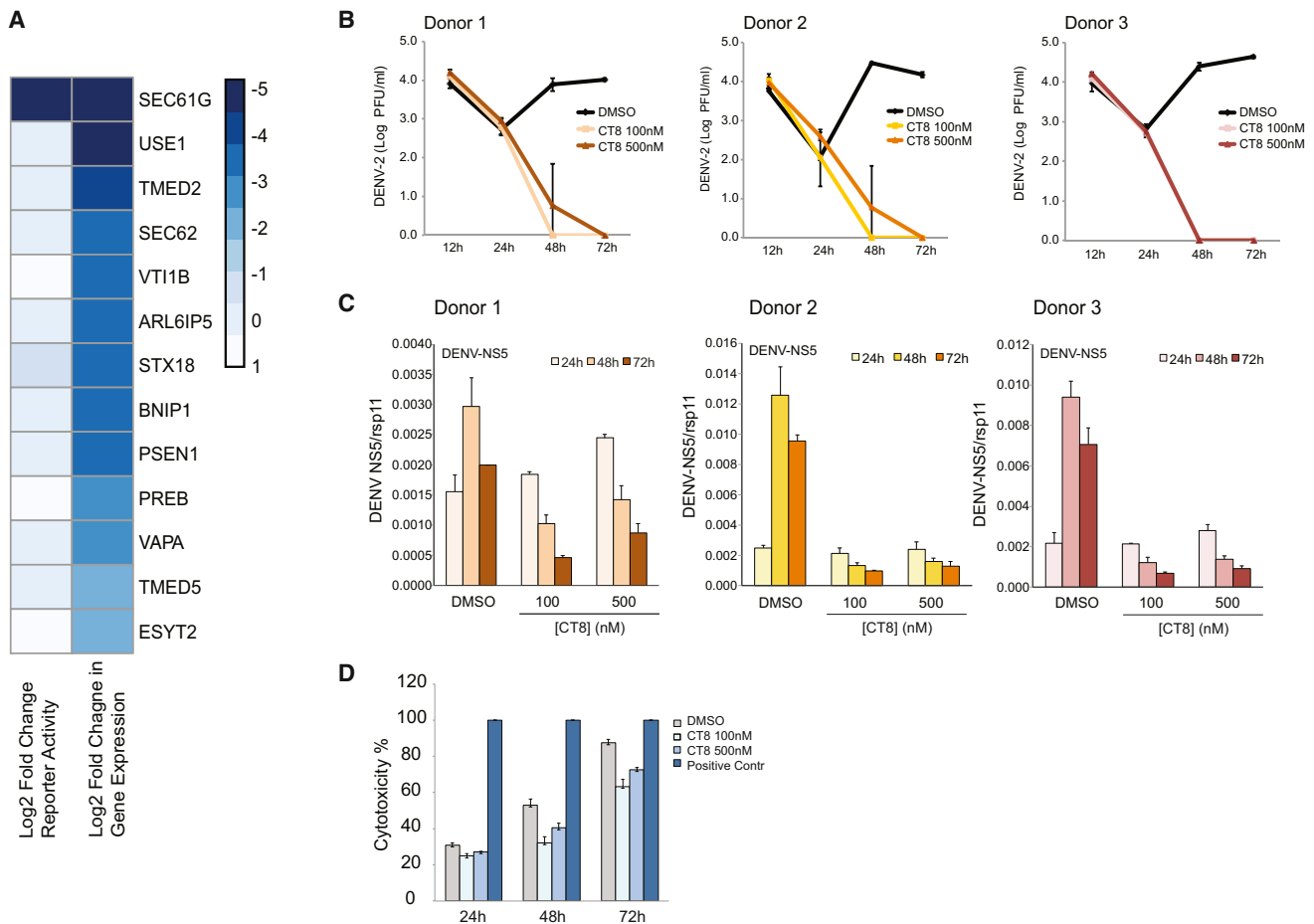
Figure 5. Sec61A Inhibition Suppresses DENV Replication

(A) Heatmap of DENV-Luc reporter replication in cells knocked down for the indicated host factors (left). Degree of knockdown of each respective factor is shown (right).

(B) Human dendritic cells from three individual donors were infected with MOCK or DENV-2 (16681) at MOI = 0.5, and total RNA was extracted at 24, 48, and 72 hr after infection. Relative expression of viral RNA was measured by qRT-PCR at specific time points normalized against rsp11.

(C) Accumulation of infectious DENV particles in the supernatant was quantified by plaque assay at 12, 24, 48, and 72 hr after infection for the three individual donors. Error bars indicate SD of the mean from duplicate samples.

(D) Macrophage-derived dendritic cells (MDDCs) were incubated with MOCK, 100 nM CT8, or 500 nM; the same final concentration of DMSO was used for the three conditions. Treatment was stopped at 24, 48, and 72 hr, and cytotoxicity was measured with the CytoTox 96 Non-Radioactive Cytotoxicity Assay (Promega). DC lysate was used as a positive control for the assay (see Supplemental Experimental Procedures). Error bars indicate SD from duplicate samples.

Sec61 Controls DENV Biogenesis and Can Be Targeted to Suppress DENV Infectivity

We then focused our attention on DENV, an emerging pathogen and a global threat that relies heavily on the ER to coordinate viral assembly and life cycle (Diamond and Pierson, 2015; Lindenbach and Rice, 1999). Because global proteomic mapping for DENV is not available, we knocked down Sec61 and 12 other factors controlling ER events (GO category 0005789) and then monitored viral replication (Figure 5A). Our analysis revealed that only Sec61 depletion resulted in suppression of DENV replication (Figure 5A). Prompted by this, we infected monocyte-derived dendritic cells (MDDCs) from three independent human donors and assessed DENV mRNA dynamics and DENV replication in the presence and absence of CT8. Our analysis showed that CT8 inhibited DENV mRNA expression and replication in a dose-dependent manner (Figures 5B and 5C) and had no effect on cell viability (Figure 5D).

DISCUSSION

We report the interaction network of influenza during an active infection event. An unbiased hierarchical clustering of the host pathways affected by each viral protein led to several functional groupings of viral proteins. This approach, analyzing protein-protein interaction datasets through an integrated view of cellular and viral complexes, can serve to identify critical cellular "nodes" which, upon disruption, could have effects on multiple viral proteins at the same time. As a validation of this method, we characterized the contribution (with respect to viral replication) of inhibiting novel nuclear and cytosolic host factors that control co-opted host pathways.

One of the major strengths of our approach, the fact that viral protein complexes like RNPs are formed during infection, also complicates the interpretation of the data. Independent purification of different viral proteins can lead to the recovery of the same viral complexes, and consequently, we observed that different samples were enriched for some of the same host factors. It is therefore difficult in certain cases to determine a unique binding partner of a particular factor, for which quantitative analysis of binary interactions might be useful (Jäger et al., 2012).

Finally, among the strengths of our strategy are that it is physiologically relevant, it can be applied to in vivo infection models, and it can reveal important cognate viral protein interactions (Kuo and Krug, 2009; Zhao et al., 2010), the molecular understanding of which could shed light on the viral genomic segment incompatibility often seen in viral re-assortment studies. Elucidating the basis of this mechanism could help with predicting the fixation of genomic segments between different species that are at the basis of increased viral pathogenicity and pandemic potential.

The host factor that we focused on in this study, Sec61A1, represents an essential host factor whose inhibition affects the proteostasis of influenza virus, HIV, DENV and potentially other viruses (Iwasa et al., 2011; Panda et al., 2013). We show that HA is highly sensitive to Sec61A1 levels, much more so than M2 or MHC-I, and that Sec61A1 inhibition leads to reduced HA trimer formation and subsequent surface expression. Interestingly, previous works have both hypothesized (Fayadat and Kopito, 2003) and shown (Pitonzo and Skach, 2006; Pitonzo et al., 2009; Skach, 2007), that Sec61-mediated translocation can directly play a role in protein folding and processing. Other works have suggested that nascent-chain-Sec61 interaction dictates cotranslational events (Conti et al., 2015). In line with these, our data show that when Sec61A1 is inhibited or its levels are reduced, a larger percentage of HA is not glycosylated and is possibly terminally misfolded. Alternatively, partially misfolded HA might still engage in oligomerization, generating aberrant trimers not detected with trimer-specific antibodies. In this case, a single misfolded monomer could "poison" two correctly folded HA proteins and generate HA trimers with defects in membrane insertion, budding, and trypsin sensitivity. Interestingly, during infection such defective HA conformers are formed constitutively in considerable amounts, previously estimated to be 10% of total HA (Copeland et al., 1986). This suggests the existence of regulators or cellular antagonists to proper HA trimerization. Strikingly, the number of defective HA trimers increases in infected cells when the activity of both Calnexin and Calreticulin is compromised (Molinari et al., 2004).

As such, alteration of glycosylation-deglycosylation kinetics and quality control, as revealed in both our current and previous studies, results in the inhibition of viral growth and underlines a unique folding requirement for viral glycoproteins (Pieren et al., 2005). The recent finding that Calnexin is in physical contact with the translocon (Lakkaraju et al., 2012) and can be regulated after short-term ER stress (Lynes et al., 2013) further supports this interpretation and indicates that signaling can regulate viral glycoproteostasis.

Another important aspect of our study is revealed by our metabolic-chase experiments in the presence of CT8. Although the more characterized consequence of Sec61 inhibition by CT8 is proteasome-dependent destruction of non-translocated substrates (Besemer et al., 2005; Garrison et al., 2005), recent pieces of evidence indicate that a delay in the initiation of translocation (as opposed to a complete block) can differentially interfere with the expression of cellular and prion proteins (Conti et al., 2015). Indeed, our results indicate that altering Sec61A1 levels results in delayed HA translocation and trimer formation.

Viral proteins whose correct folding and ER exit require oligomerization, e.g., HA and NA, (Ceriotti and Colman, 1990; Copeland et al., 1988; Hogue and Nayak, 1992; Saito et al., 1995; Wang et al., 2008), might be highly sensitive to the net flux into the ER and therefore to Sec61 activity. When the flux of protein translocation is reduced, HA monomers might fall into a kinetic trap whereby they enter a terminally misfolded state. In support of this hypothesis, previous reports show that HA oligomeric assembly is dependent on the expression level of HA, whereas the rate of folding is independent from it (Braakman et al., 1991; Ceriotti and Colman, 1990). This observation would also explain why, during infection, highly expressed viral oligomeric proteins are preferentially affected by the amount of Sec61. In agreement with this, HIV-1 gp160/gp120 is also known to oligomerize before ER exit (Earl et al., 1990; Earl et al., 1991; Land et al., 2003) and shows the same sensitivity to the reduced amount of Sec61A1 or CT8 treatment. In line with this model, M2 and MHC-I are not known to have an ER oligomerization requirement.

How can the inhibition of an essential cell function be a valid antiviral therapy? Overall, our data indicate that the viral biogenesis of DENV, HIV, and IAV is regulated by the amount of Sec61 and, as such, Sec61 chemical inhibition can suppress viral growth with little to no effect on cellular homeostasis. This is most likely the result of both the unique requirement for viral glycoprotein folding and maturation (Pieren et al., 2005) and the fact that, unlike the majority of cellular proteins, viral proteins rely on high synthetic rates and high expression levels during the short time frame of acute infection (Braakman et al., 1991; Ceriotti and Colman, 1990). The advantage of using, for the purpose of containing an infection, inhibitors such as the one described here (CT8) and others that lead to derailment of N-linked glycoprotein maturation (i.e., glucosyl inhibitors; see reviews [Dalziel et al., 2014; Hebert et al., 2014]) stands on the intrinsic requirements of viral life cycles. Thus, transient (and partial) inhibition of an essential cell function becomes particularly detrimental for the synthesis of viral proteins and viral biogenesis, whereas it is well tolerated by the host cell. In our case, a CT8-substrate-specific effect on HA seems to be present and is probably dependent on the substrate's primary sequence. Along this line, inhibitors of protein translocation across the ER membrane have been developed and display partial substrate specificities and allosteric effects on many targets (Kalies and Römisch, 2015). Because virus can mutagenize their proteins easily, retaining broad inhibitory capacity of chemical features (i.e., hydrophobicity of signal peptide) could be advantageous with respect to specific inhibitors with one substrate.

In essence, the infectious-based strategy delineated here is potentially applicable to any virus to guide (1) functional studies, (2) the analysis of disease-disease relationship and the identification of common targets for inhibition of multiple viruses, and (3) the search for novel antiviral therapies.

In conclusion, we provide a path and a biologically relevant approach to studying the interplay between viruses and their hosts.

EXPERIMENTAL PROCEDURES

293T, A549 and MDCK cells (American Type Culture Collection) were primarily used with respect to influenza virus studies. For HIV-1 experiments, the cell lines A3R5.7 and TZM-bl, were obtained from the NIH AIDS Reagent Program. We used human DC in the studies of DENV replication (see Supplemental Experimental Procedures). All cells were maintained in DMEM supplemented with 10% fetal calf serum, L-glutamine, penicillin, and streptomycin. Cells were routinely checked for contamination with MycoAlert (Lonza). For infection, we diluted virus in PBS supplemented with 3% BSA and used it to infect cells for 1 hr at 37°C, after which we replaced the culture media. For multi-cycle growth curves, MDCK cells were infected at an MOI of 0.001. For determination of titer, virus was plaqued on MDCK cells as previously described (Heaton et al., 2013a).

Cloning and Rescue of Flag-Tagged Viruses

Flag epitopes were introduced into the viral coding regions in the ambisense pDZ vector. Flag-epitope insertion was achieved by insertion of the Flag sequence into overlapping primers and InfusionHD cloning (Clontech). Insertion sites were cloned in after the following nucleotides (existing amino acids were used wherever possible): HA-Flag; 437, NA-Flag; 206, NS1-Flag; 515, NEP-Flag; 531, M2-Flag; 800, PA-Flag, PB1-Flag, PB2-Flag expressing the Flag epitope on the C terminus and including duplicated RNA packaging signals of 184, 160, and 169 nucleotides, respectively. In cases where a packaging signal was duplicated, the original packaging signal was eliminated via the introduction of silent mutations. The insertion sites are based on the sequences of the viral segments corresponding to GenBank accession numbers AF389115, AF389116, AF389117, AF389118, AF389119, AF389120, AF389121, and AF389122. Clone sequences were verified and rescued via 293T transfection and amplification in embryonated chicken eggs. In all cases, viruses were plaque or dilution purified. RT-PCR and sequencing of viral stocks was used for confirmation of Flag-epitope insertion in rescued viruses.

Immunoprecipitation and Mass Spectrometry

We employed an Ap-ms strategy similar to (Miller et al., 2015). Briefly, for each Flag-influenza protein purification, 4×10^8 were infected for 10 hr at an MOI = 3, collected and lyzed in 20 ml of cold lysis buffer (0.2% NP40, 50 mM Tris–HCl pH 7.5; 150 mM NaCl, 1 mM EDTA, protease and phosphatase inhibitors). Douncing and mild sonication (5 cycle 30'ON/OFF with Diagenode Bioruptor) were followed by Centrifugation for 30' at 13K. The supernatant was precleared with dynabeads (No Ab) for 2h at 4C. To the precleared extract, 300 μl of Flag-dynabeads were added and incubated for 2 hr at 4°C to allow immunoprecipitation of Flag-bound complexes. After 6 washes in Wash Buffer (0.2% NP40, 50 mM Tris–HCl pH 7.5, 200 mM NaCl, 1 mM EDTA), 2 extra washes were conducted in no-detergent wash buffer. Immunocomplexes were then eluted with 3xFlag-peptide with 100 μg/ml of 3xFlag peptide (3 elution of 15' each). Eluted material was then precipitated overnight with acetone. A brief spin (13K for 15 s) was used to pellet the precipitated proteins that were then resolubilized, trypsin-digested and subjected to ms-ms.

Mass Spectrometry Analysis

Samples were analyzed by the Proteomics Resource Center at The Rockefeller University. Proteins were denatured, reduced, alkylated, and proteolytically digested with endoproteinase LysC (Wako Chemicals), and subsequently with trypsin (Promega). Peptides were desalted and analyzed by reversed-phase nano-HPLC-MS/MS (Ultimate 3000 coupled to QExactive from Thermo Scientific). Data were extracted and searched against the Human Uniprot database with Proteome Discoverer 1.4 (Thermo Scientific) and Mascot 2.4 (Matrix Science). Identified peptides were filtered with a 1% false discovery rate and Percolator (Käll et al., 2007). In the table, proteins are sorted according to their relative abundance, which is represented by the peak area. The protein area was calculated by the software as an average of the areas of the three most abundant peptides for that protein.

See also Supplemental Experimental Procedures for detailed protocols.

REFERENCES

Alsuwaidi, A.R., Almarzooqi, S., Albawardi, A., Benedict, S., Kochiyil, J., Mustafa, F., Hartwig, S.M., Varga, S.M., and Souid, A.K. (2013). Cellular bioenergetics, caspase activity and glutathione in murine lungs infected with influenza A virus. Virology 446, 180–188.

Amorim, M.J., Read, E.K., Dalton, R.M., Medcalf, L., and Digard, P. (2007). Nuclear export of influenza A virus mRNAs requires ongoing RNA polymerase II activity. Traffic 8, 1–11.

Besemer, J., Harant, H., Wang, S., Oberhauser, B., Marquardt, K., Foster, C.A., Schreiner, E.P., de Vries, J.E., Dascher-Nadel, C., and Lindley, I.J.D. (2005). Selective inhibition of cotranslational translocation of vascular cell adhesion molecule 1. Nature 436, 290–293.

Braakman, I., Hoover-Litty, H., Wagner, K.R., and Helenius, A. (1991). Folding of influenza hemagglutinin in the endoplasmic reticulum. J. Cell Biol. 114, 401–411.

Bradel-Tretheway, B.G., Mattiacio, J.L., Krasnoselsky, A., Stevenson, C., Purdy, D., Dewhurst, S., and Katze, M.G. (2011). Comprehensive proteomic

analysis of influenza virus polymerase complex reveals a novel association with mitochondrial proteins and RNA polymerase accessory factors. J. Virol. *85*, 8569–8581.

Caramelo, J.J., and Parodi, A.J. (2008). Getting in and out from calnexin/calreticulin cycles. J. Biol. Chem. *283*, 10221–10225.

Ceriotti, A., and Colman, A. (1990). Trimer formation determines the rate of influenza virus haemagglutinin transport in the early stages of secretion in Xenopus oocytes. J. Cell Biol. *111*, 409–420.

Chakrabarti, L.A., Ivanovic, T., and Cheng-Mayer, C. (2002). Properties of the surface envelope glycoprotein associated with virulence of simian-human immunodeficiency virus SHIV(SF33A) molecular clones. J. Virol. *76*, 1588–1599.

Conti, B.J., Devaraneni, P.K., Yang, Z., David, L.L., and Skach, W.R. (2015). Cotranslational stabilization of Sec62/63 within the ER Sec61 translocon is controlled by distinct substrate-driven translocation events. Mol. Cell *58*, 269–283.

Copeland, C.S., Doms, R.W., Bolzau, E.M., Webster, R.G., and Helenius, A. (1986). Assembly of influenza hemagglutinin trimers and its role in intracellular transport. J. Cell Biol. *103*, 1179–1191.

Copeland, C.S., Zimmer, K.P., Wagner, K.R., Healey, G.A., Mellman, I., and Helenius, A. (1988). Folding, trimerization, and transport are sequential events in the biogenesis of influenza virus hemagglutinin. Cell *53*, 197–209.

Dalziel, M., Crispin, M., Scanlan, C.N., Zitzmann, N., and Dwek, R.A. (2014). Emerging principles for the therapeutic exploitation of glycosylation. Science *343*, 1235681.

Daniels, R., Kurowski, B., Johnson, A.E., and Hebert, D.N. (2003). N-linked glycans direct the cotranslational folding pathway of influenza hemagglutinin. Mol. Cell *11*, 79–90.

de Chassey, B., Aublin-Gex, A., Ruggieri, A., Meyniel-Schicklin, L., Pradezynski, F., Davoust, N., Chantier, T., Tafforeau, L., Mangeot, P.E., Ciancia, C., et al. (2013). The interactomes of influenza virus NS1 and NS2 proteins identify new host factors and provide insights for ADAR1 playing a supportive role in virus replication. PLoS Pathog. *9*, e1003440.

Diamond, M.S., and Pierson, T.C. (2015). Molecular Insight into Dengue Virus Pathogenesis and Its Implications for Disease Control. Cell *162*, 488–492.

Divakaruni, A.S., and Murphy, A.N. (2012). Cell biology. A mitochondrial mystery, solved. Science *337*, 41–43.

Earl, P.L., Doms, R.W., and Moss, B. (1990). Oligomeric structure of the human immunodeficiency virus type 1 envelope glycoprotein. Proc. Natl. Acad. Sci. USA *87*, 648–652.

Earl, P.L., Moss, B., and Doms, R.W. (1991). Folding, interaction with GRP78-BiP, assembly, and transport of the human immunodeficiency virus type 1 envelope protein. J. Virol. *65*, 2047–2055.

Engelhardt, O.G., Smith, M., and Fodor, E. (2005). Association of the influenza A virus RNA-dependent RNA polymerase with cellular RNA polymerase II. J. Virol. *79*, 5812–5818.

Fayadat, L., and Kopito, R.R. (2003). Recognition of a single transmembrane degron by sequential quality control checkpoints. Mol. Biol. Cell *14*, 1268–1278.

Fislová, T., Thomas, B., Graef, K.M., and Fodor, E. (2010). Association of the influenza virus RNA polymerase subunit PB2 with the host chaperonin CCT. J. Virol. *84*, 8691–8699.

García-Sastre, A., and Palese, P. (1993). Genetic manipulation of negative-strand RNA virus genomes. Annu. Rev. Microbiol. *47*, 765–790.

Garrison, J.L., Kunkel, E.J., Hegde, R.S., and Taunton, J. (2005). A substrate-specific inhibitor of protein translocation into the endoplasmic reticulum. Nature *436*, 285–289.

Gogala, M., Becker, T., Beatrix, B., Armache, J.P., Barrio-Garcia, C., Berninghausen, O., and Beckmann, R. (2014). Structures of the Sec61 complex engaged in nascent peptide translocation or membrane insertion. Nature *506*, 107–110.

Gorai, T., Goto, H., Noda, T., Watanabe, T., Kozuka-Hata, H., Oyama, M., Takano, R., Neumann, G., Watanabe, S., and Kawaoka, Y. (2012). F1Fo-ATPase, F-type proton-translocating ATPase, at the plasma membrane is critical for efficient influenza virus budding. Proc. Natl. Acad. Sci. USA *109*, 4615–4620.

Grasberger, B., Minton, A.P., DeLisi, C., and Metzger, H. (1986). Interaction between proteins localized in membranes. Proc. Natl. Acad. Sci. USA *83*, 6258–6262.

Guan, Z.H., Zhang, M.L., Hou, P.L., Duan, M., Cui, Y.M., and Wang, X.R. (2012). Identification of cellular proteins interacting with influenza A virus PB1-F2 protein. Acta Virol. *56*, 199–207.

Hale, B.G., Randall, R.E., Ortín, J., and Jackson, D. (2008). The multifunctional NS1 protein of influenza A viruses. J. Gen. Virol. *89*, 2359–2376.

Halestrap, A.P. (2012). The mitochondrial pyruvate carrier: has it been unearthed at last? Cell Metab. *16*, 141–143.

Heaton, N.S., Leyva-Grado, V.H., Tan, G.S., Eggink, D., Hai, R., and Palese, P. (2013a). In vivo bioluminescent imaging of influenza a virus infection and characterization of novel cross-protective monoclonal antibodies. J. Virol. *87*, 8272–8281.

Heaton, N.S., Sachs, D., Chen, C.J., Hai, R., and Palese, P. (2013b). Genome-wide mutagenesis of influenza virus reveals unique plasticity of the hemagglutinin and NS1 proteins. Proc. Natl. Acad. Sci. USA *110*, 20248–20253.

Hebert, D.N., Zhang, J.X., Chen, W., Foellmer, B., and Helenius, A. (1997). The number and location of glycans on influenza hemagglutinin determine folding and association with calnexin and calreticulin. J. Cell Biol. *139*, 613–623.

Hebert, D.N., Lamriben, L., Powers, E.T., and Kelly, J.W. (2014). The intrinsic and extrinsic effects of N-linked glycans on glycoproteostasis. Nat. Chem. Biol. *10*, 902–910.

Heiny, A.T., Miotto, O., Srinivasan, K.N., Khan, A.M., Zhang, G.L., Brusic, V., Tan, T.W., and August, J.T. (2007). Evolutionarily conserved protein sequences of influenza a viruses, avian and human, as vaccine targets. PLoS ONE *2*, e1190.

Hogue, B.G., and Nayak, D.P. (1992). Synthesis and processing of the influenza virus neuraminidase, a type II transmembrane glycoprotein. Virology *188*, 510–517.

Iwasa, A., Halfmann, P., Noda, T., Oyama, M., Kozuka-Hata, H., Watanabe, S., Shimojima, M., Watanabe, T., and Kawaoka, Y. (2011). Contribution of Sec61α to the life cycle of Ebola virus. J. Infect. Dis. *204* (*Suppl 3*), S919–S926.

Jäger, S., Gulbahce, N., Cimermancic, P., Kane, J., He, N., Chou, S., D'Orso, I., Fernandes, J., Jang, G., Frankel, A.D., et al. (2011). Purification and characterization of HIV-human protein complexes. Methods *53*, 13–19.

Jäger, S., Cimermancic, P., Gulbahce, N., Johnson, J.R., McGovern, K.E., Clarke, S.C., Shales, M., Mercenne, G., Pache, L., Li, K., et al. (2012). Global landscape of HIV-human protein complexes. Nature *481*, 365–370.

Jorba, N., Juarez, S., Torreira, E., Gastaminza, P., Zamarreño, N., Albar, J.P., and Ortín, J. (2008). Analysis of the interaction of influenza virus polymerase complex with human cell factors. Proteomics *8*, 2077–2088.

Kalies, K.U., and Römisch, K. (2015). Inhibitors of Protein Translocation Across the ER Membrane. Traffic *16*, 1027–1038.

Käll, L., Canterbury, J.D., Weston, J., Noble, W.S., and MacCoss, M.J. (2007). Semi-supervised learning for peptide identification from shotgun proteomics datasets. Nat. Methods *4*, 923–925.

Kuo, R.L., and Krug, R.M. (2009). Influenza a virus polymerase is an integral component of the CPSF30-NS1A protein complex in infected cells. J. Virol. *83*, 1611–1616.

Lakkaraju, A.K., Abrami, L., Lemmin, T., Blaskovic, S., Kunz, B., Kihara, A., Dal Peraro, M., and van der Goot, F.G. (2012). Palmitoylated calnexin is a key component of the ribosome-translocon complex. EMBO J. *31*, 1823–1835.

Land, A., Zonneveld, D., and Braakman, I. (2003). Folding of HIV-1 envelope glycoprotein involves extensive isomerization of disulfide bonds and conformation-dependent leader peptide cleavage. FASEB J. *17*, 1058–1067.

Lin, L., Li, Y., Pyo, H.M., Lu, X., Raman, S.N.T., Liu, Q., Brown, E.G., and Zhou, Y. (2012). Identification of RNA helicase A as a cellular factor that interacts with influenza A virus NS1 protein and its role in the virus life cycle. J. Virol. *86*, 1942–1954.

Lindenbach, B.D., and Rice, C.M. (1999). Genetic interaction of flavivirus nonstructural proteins NS1 and NS4A as a determinant of replicase function. J. Virol. 73, 4611–4621.

Lue, J., Hsu, M., Yang, D., Marx, P., Chen, Z., and Cheng-Mayer, C. (2002). Addition of a single gp120 glycan confers increased binding to dendritic cell-specific ICAM-3-grabbing nonintegrin and neutralization escape to human immunodeficiency virus type 1. J. Virol. 76, 10299–10306.

Lynes, E.M., Raturi, A., Shenkman, M., Ortiz Sandoval, C., Yap, M.C., Wu, J., Janowicz, A., Myhill, N., Benson, M.D., Campbell, R.E., et al. (2013). Palmitoylation is the switch that assigns calnexin to quality control or ER Ca2+ signaling. J. Cell Sci. 126, 3893–3903.

Mackinnon, A.L., Paavilainen, V.O., Sharma, A., Hegde, R.S., and Taunton, J. (2014). An allosteric Sec61 inhibitor traps nascent transmembrane helices at the lateral gate. eLife 3, e01483.

Mayer, D., Molawi, K., Martínez-Sobrido, L., Ghanem, A., Thomas, S., Baginsky, S., Grossmann, J., García-Sastre, A., and Schwemmle, M. (2007). Identification of cellular interaction partners of the influenza virus ribonucleoprotein complex and polymerase complex using proteomic-based approaches. J. Proteome Res. 6, 672–682.

Menche, J., Sharma, A., Kitsak, M., Ghiassian, S.D., Vidal, M., Loscalzo, J., and Barabási, A.L. (2015). Disease networks. Uncovering disease-disease relationships through the incomplete interactome. Science 347, 1257601.

Miller, M.S., Rialdi, A., Ho, J.S., Tilove, M., Martinez-Gil, L., Moshkina, N.P., Peralta, Z., Noel, J., Melegari, C., Maestre, A.M., et al. (2015). Senataxin suppresses the antiviral transcriptional response and controls viral biogenesis. Nat. Immunol. 16, 485–494.

Molinari, M., Eriksson, K.K., Calanca, V., Galli, C., Cresswell, P., Michalak, M., and Helenius, A. (2004). Contrasting functions of calreticulin and calnexin in glycoprotein folding and ER quality control. Mol. Cell 13, 125–135.

Munier, S., Rolland, T., Diot, C., Jacob, Y., and Naffakh, N. (2013). Exploration of binary virus-host interactions using an infectious protein complementation assay. Mol. Cell. Proteomics 12, 2845–2855.

Ngamurulert, S., Limjindaporn, T., and Auewaraku, P. (2009). Identification of cellular partners of Influenza A virus (H5N1) non-structural protein NS1 by yeast two-hybrid system. Acta Virol. 53, 153–159.

Noton, S.L., Medcalf, E., Fisher, D., Mullin, A.E., Elton, D., and Digard, P. (2007). Identification of the domains of the influenza A virus M1 matrix protein required for NP binding, oligomerization and incorporation into virions. J. Gen. Virol. 88, 2280–2290.

Panda, D., Rose, P.P., Hanna, S.L., Gold, B., Hopkins, K.C., Lyde, R.B., Marks, M.S., and Cherry, S. (2013). Genome-wide RNAi screen identifies SEC61A and VCP as conserved regulators of Sindbis virus entry. Cell Rep. 5, 1737–1748.

Paterson, D., and Fodor, E. (2012). Emerging roles for the influenza A virus nuclear export protein (NEP). PLoS Pathog. 8, e1003019.

Pieren, M., Galli, C., Denzel, A., and Molinari, M. (2005). The use of calnexin and calreticulin by cellular and viral glycoproteins. J. Biol. Chem. 280, 28265–28271.

Pitonzo, D., and Skach, W.R. (2006). Molecular mechanisms of aquaporin biogenesis by the endoplasmic reticulum Sec61 translocon. Biochim. Biophys. Acta 1758, 976–988.

Pitonzo, D., Yang, Z., Matsumura, Y., Johnson, A.E., and Skach, W.R. (2009). Sequence-specific retention and regulated integration of a nascent membrane protein by the endoplasmic reticulum Sec61 translocon. Mol. Biol. Cell 20, 685–698.

Portela, A., and Digard, P. (2002). The influenza virus nucleoprotein: a multifunctional RNA-binding protein pivotal to virus replication. J. Gen. Virol. 83, 723–734.

Ritter, J.B., Wahl, A.S., Freund, S., Genzel, Y., and Reichl, U. (2010). Metabolic effects of influenza virus infection in cultured animal cells: Intra- and extracellular metabolite profiling. BMC Syst. Biol. 4, 61.

Saito, T., Taylor, G., and Webster, R.G. (1995). Steps in maturation of influenza A virus neuraminidase. J. Virol. 69, 5011–5017.

Schneider-Schaulies, J., and Schneider-Schaulies, S. (2015). Sphingolipids in viral infection. Biol. Chem. 396, 585–595.

Schnell, D.J., and Hebert, D.N. (2003). Protein translocons: multifunctional mediators of protein translocation across membranes. Cell 112, 491–505.

Shapira, S.D., Gat-Viks, I., Shum, B.O., Dricot, A., de Grace, M.M., Wu, L., Gupta, P.B., Hao, T., Silver, S.J., Root, D.E., et al. (2009). A physical and regulatory map of host-influenza interactions reveals pathways in H1N1 infection. Cell 139, 1255–1267.

Shaw, M.L., and Palese, P. (2013). Orthomyxoviruses. In Fields Virology, D.M. Knipe and P.M. Howley, eds. (Philadelphia: Lippincott Williams and Wilkins), pp. 1151–1185.

Skach, W.R. (2007). The expanding role of the ER translocon in membrane protein folding. J. Cell Biol. 179, 1333–1335.

Tafforeau, L., Chantier, T., Pradezynski, F., Pellet, J., Mangeot, P.E., Vidalain, P.O., Andre, P., Rabourdin-Combe, C., and Lotteau, V. (2011). Generation and comprehensive analysis of an influenza virus polymerase cellular interaction network. J. Virol. 85, 13010–13018.

Wang, N., Glidden, E.J., Murphy, S.R., Pearse, B.R., and Hebert, D.N. (2008). The cotranslational maturation program for the type II membrane glycoprotein influenza neuraminidase. J. Biol. Chem. 283, 33826–33837.

Watanabe, T., Kawakami, E., Shoemaker, J.E., Lopes, T.J., Matsuoka, Y., Tomita, Y., Kozuka-Hata, H., Gorai, T., Kuwahara, T., Takeda, E., et al. (2014). Influenza virus-host interactome screen as a platform for antiviral drug development. Cell Host Microbe 16, 795–805.

Zhao, C., Kuo, R.-L., and Krug, R.M. (2010). The NS1 Protein of Influenza A Virus. In Influenza: Molecular Virology, Q. Wang and Y.J. Tao, eds. (Norfolk, UK: Caister Academic Press), pp. 1–14.